# Characterizing passive coherent population trapping resonance in a cesium vapor cell filled with neon buffer gas*

Liu Zhi(刘 智), Wang Jie-Ying(王杰英), Diao Wen-Ting(刁文婷), He Jun(何 军), and Wang Jun-Min(王军民)†

*State Key Laboratory of Quantum Optics and Quantum Optics Devices (Shanxi University), and Institute of Opto-Electronics, Shanxi University, Taiyuan* 030006, *China*

(Received 7 December 2012; revised manuscript received 11 January 2013)

We present a pair of phase-locked lasers with a 9.2-GHz frequency difference through the injection locking of a master laser to the RF-modulation sideband of a slave diode laser. Using this laser system, a coherent population trapping (CPT) signal with a typical linewidth of ∼ 182 Hz is obtained in a cesium vapor cell filled with 30 Torr (4 kPa) of neon as the buffer gas. We investigate the influence of the partial pressure of the neon buffer gas on the CPT linewidth, amplitude, and frequency shift. The results may offer some references for CPT atomic clocks and CPT atomic magnetometers.

**Keywords:** coherent population trapping (CPT), phase locking of two-color lasers, cesium (Cs) vapor cell, buffer gas

**PACS:** 32.70.Jz, 32.80.Pj, 32.80.Qk **DOI:** 10.1088/1674-1056/22/4/043201

## 1. Introduction

A pair of phase-locked laser fields is used to couple the two hyperfine ground state levels and one excited state hyperfine level of alkali metal atoms, which causes the Lambda-type three-level atoms to be driven in a superposition dark state and the photons to not be absorbed anymore. Coherence between the two ground states is established. This coherence creates an oscillating magnetization that can be detected directly through stimulated emission in a cavity (active mode). A narrow dark line in the fluorescence spectrum or a narrow increased transmission peak can also be observed (passive mode). This is called the coherent population trapping (CPT) effect. It was first observed in 1976,[1] and then because of the very narrow resonance lines was proposed to be used for atom cooling,[2] high-sensitivity magnetometers,[3–5] and atomic clocks.[6–10]

For better application, people need to obtain a greater amplitude[11] and narrower linewidth (the full-width at half-maximum (FWHM)).[12] The linewidth of CPT resonance ($\Delta\upsilon$) is limited by the interaction time and laser power broadening.[6] So techniques for extending the atomic coherence time, proper buffer gas or paraffin coating in atomic vapor cells are usually adopted. We have previously used a cesium (Cs) vapor cell filled with 2-Torr (267 Pa) neon (Ne) to narrow the linewidth significantly.[13] On the basis of our previous work, in this paper we experimentally measure and theoretically analyze the different partial pressures of Ne serving as the buffer gas for the Cs atoms' passive CPT characteristics. The linewidth, amplitude, and center frequency shift effects are studied at room temperature, and we further obtain a much narrower linewidth (∼ 182 Hz) in a Cs vapor cell filled with 30-Torr (4 kPa) Ne gas.

## 2. Experimental setup

According to the current reports, the large frequency difference (∼ GHz) and phase-locked lasers are usually realized by the following methods: 1) directly modulating the vertical cavity surface emitting laser (VCSEL) current by using ±1-order sidebands or the carrier and one of the first-order sidebands;[14] 2) shifting the frequency of the incident laser through the acousto–optic modulator (AOM) that works in the high-frequency regime,[15] or using a higher order diffracted beam and the zero-order beam of the AOM;[16] 3) using a broadband electronic feedback loop to make two lasers that are phase-locked through the beat-note signal;[17] and 4) using the indirect optical injection locking method to lock the phase between the master laser and slave laser.[18,19] The above methods have their own advantages and disadvantages, and the method we will adopt in this paper is slightly different. Our method of optical and electrical circuits is relatively simple, and can adjust the strengths of the two coherent lights arbitrarily. Figure 1 shows our experimental setup for CPT in a Lambda-type system ($6S_{1/2}$ ($F_g = 3$) and $6S_{1/2}$ ($F_g = 4$)–$6P_{3/2}$ ($F_e = 4$) of $^{133}$Cs). We use a direct injection-locking scheme to produce two phase-locked lasers.[20] The master laser (ML) is a home-made 852 nm extended-cavity diode laser (ECDL), and has a typical output power of about 60 mW

*Project supported by the National Natural Science Foundation of China (Grant Nos. 11274213, 61205215, 61078051, and 612279002), the National Major Scientific Research Program of China (Grant No. 2012CB921601), the Research Project for Returned Abroad Scholars from Universities of Shanxi Province, China (Grant No. 2012-015), and the Project for Excellent Research Team of the National Natural Science Foundation of China (Grant No. 61121064).

†Corresponding author. E-mail: wwjjmm@sxu.edu.cn

© 2013 Chinese Physical Society and IOP Publishing Ltd 

with a linewidth of $\sim$ 500 kHz (in 50 ms). Using a saturation absorption spectroscopic (SAS) scheme, we fix the ML to the frequency corresponding to the Cs $F_g = 3$–$F_e = 4$ hyperfine transition of the Cs $D_2$ line. The slave laser (SL) is a single-mode 9 mm-can-packaged Fabry–Perot-type GaAlAs semiconductor laser (JDSU 5411-G1), and its typical output power is $\sim$ 100 mW. The $\sim$ 9.193 GHz radio frequency (RF) modulation signal of a low-phase-noise RF function generator (Agilent 8257C) is applied directly to SL by a bias-Tee (Picosecond Pulse Labs, model 5547). A typical positive (or negative) first-order modulation sideband is below 6% of the SL output power when the $\sim$ 9.193 GHz RF power is +17 dBm. Part of the ML output beam is injected into the SL positive first-order sideband for optical injection locking (the polarization direction of injection light is consistent with the output light because of the half-wave plate ($\lambda/2$) and optical isolator (OI) in front of the SL). At this time, the SL carrier just works at the Cs Fg = 4–Fe = 4 hyperfine transition, and matches the ground level splitting of a Cs atom, with the frequency deviation from ML being $\sim$ 9.193 GHz. The frequency can be easily scanned around 9.193 GHz, but the injection locking is still maintained.

The laser beams are superposed on a polarization beam splitter (PBS) cube, and the intensities of the two light beams can be controlled with two $\lambda/2$ before it. Then, a $\lambda/2$ wave plate and a PBS make the polarization directions of the two phase-locked beams consistent, and the two light beams pass through a polarization-maintaining (PM) fiber, so they have clean and perfectly overlapped Gaussian profiles. Both beams are circularly polarized by a $\lambda/4$ wave plate and pass through a Cs vapor cell. The transmitted signal is detected on a photodiode. The Cs vapor cell is placed inside a three-layer $\mu$-metal magnetic shielding tank with a typical residual field of $\sim$ 1 nT.

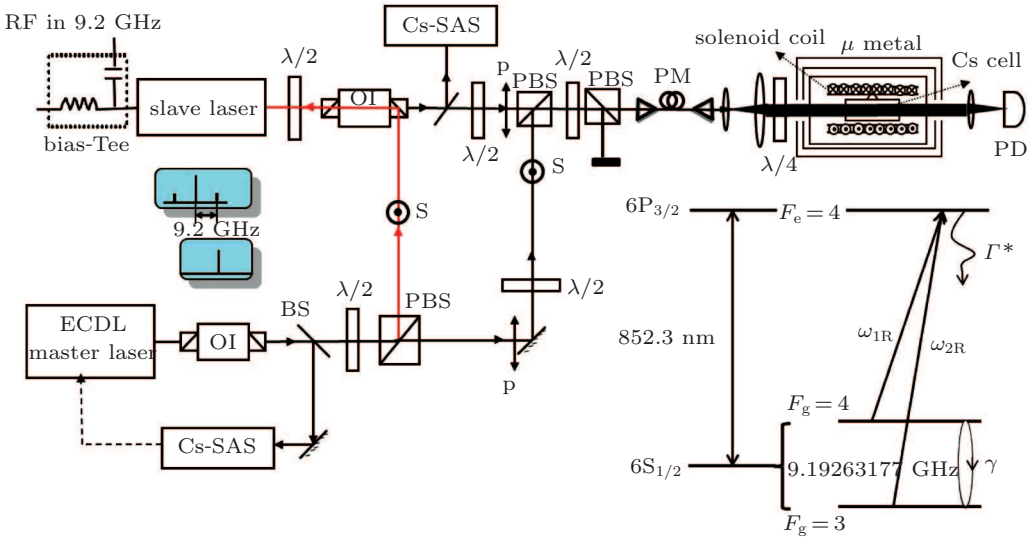



**Fig. 1.** (color online) Experimental setup used to observe narrow coherent population trapping resonances. ECDL: extended-cavity diode laser, OI: optical isolator, Cs-SAS: Cs saturation absorption spectroscopy, BS: beam splitter plate, PBS: polarizing beam splitter cube, $\lambda/2$: half-wave plate, $\lambda/4$: quarter-wave plate, S: s-polarization, P: p-polarization, PD: photodiode. The inset shows the relevant atomic energy levels.

## 3. Experimental results and discussion

### 3.1. The linewidth and amplitude of the CPT signal versus the partial pressure of the Ne buffer gas and laser intensity

The Gaussian radius ($1/e^2$) of the two phase-locked laser beams becomes $\sim$ 7.9 mm through a beam-expanding telescope, and both then pass through the Cs cell, which is placed in the magnetic shielding tank at room temperature. In our experiment, we use several Cs vapor cells filled with different partial pressure Ne as the buffer gas. The Cs vapor cells have the dimensions $\phi$25 mm$\times$75 mm. Of them, one is the pure Cs vapor cell, and four Cs cells are additionally filled with 2, 10, 20, and 30 Torr (267 Pa, 1.3 kPa, 2.7 kPa, 4 kPa) Ne as the buffer gas, respectively. Figure 2 shows two typical Lambda-type CPT resonance transmission signals of the $6S_{1/2}$–$6P_{3/2}$ transition of Cs. The linewidth for a pure Cs vapor cell is $\sim$ 18 kHz (Fig. 2(a)) and that for a Cs+30 Torr (4 kPa) Ne vapor cell is $\sim$ 182 Hz (Fig. 2(b)). However, the laser intensities of two incident beams are $I_{ML} = I_{SL} = 5$ μW/cm$^2$ for the pure Cs vapor cell, and $I_{ML} = I_{SL} = 2.5$ μW/cm$^2$ for the Cs +30 Torr (4 kPa) Ne vapor cell.

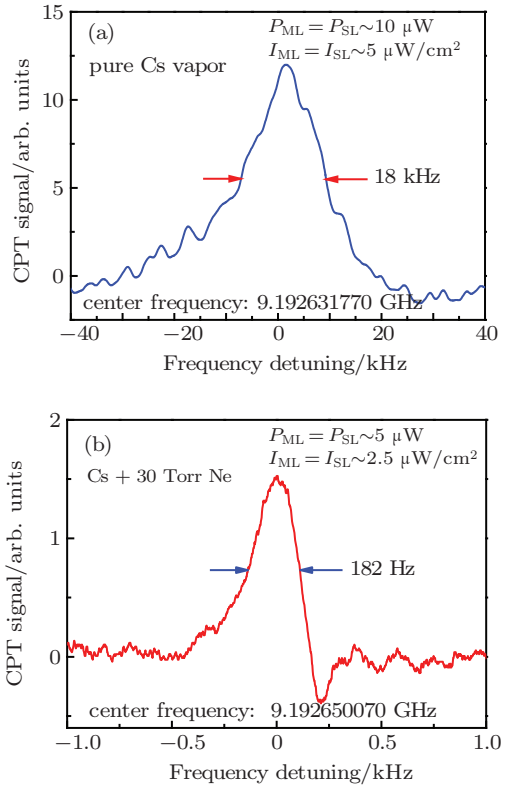



**Fig. 2.** (color online) (a) The typical CPT signal in a pure Cs vapor cell. The linewidth of the CPT resonance peak is ∼ 18 kHz. (b) A typical CPT signal in a Cs vapor cell filled with 30 Torr (4 kPa) of Ne as the buffer gas. The linewidth of the CPT resonance peak is ∼ 182 Hz.

Based on the Lambda-type three-level system, the linewidth $\Delta\upsilon$ and amplitude $S$ of the CPT signal can be expressed, respectively, as[6]

$$\Delta\upsilon = \frac{1}{\pi}\left(\gamma + \frac{\omega_{1R}^2 + \omega_{2R}^2}{2\Gamma^*}\right), \tag{1}$$

$$S \propto \frac{\omega_{1R}^2 \omega_{2R}^2}{\Gamma^*} \cdot \frac{1}{\gamma + \dfrac{\omega_{1R}^2 + \omega_{2R}^2}{2\Gamma^*}}. \tag{2}$$

Here, the Rabi angular frequencies $\omega_{1R}$ and $\omega_{2R}$ are determined by the laser intensity, $\omega_R = 2\pi \cdot \Gamma^* \cdot \sqrt{I/2I_s}$, in which $\Gamma^*$ is the total decay rate from the excited state $F_e = 4$ to the two ground levels $F_g = 3$ and $F_g = 4$, and is affected by spontaneous emission and collisions between atoms and the buffer gas. $\gamma$ is the ground state relaxation rate, which is affected by collisions between atoms and the buffer gas (the coherence in the ground states tends to zero at the $\gamma$ rate that is essentially the same as the rate at which the population of the ground levels tend to equilibrium).[6] The resonance strength $S$ depends on the atomic population in the superposition dark state.

In the case of weak intensity, the coherence relaxation rate $\gamma$ dominantly affects the CPT linewidth. It can be seen that the variation in the buffer gas pressure is caused by the change of $\gamma$:[6]

$$\gamma = \left[(2.4/a)^2 + (\pi/l)^2\right] D_0 (P_0/P) + L_0 \cdot \bar{\nu}_{rbg} \cdot g \cdot \sigma_{2bg} (P/P_0) + \gamma_{se}. \tag{3}$$

Here, $D_0$ is the diffusion constant in the cylindrical Cs atomic vapor cell that has a length of $l$, diameter of $a$ and contains the buffer gas with a partial pressure $P$. $P_0$ denotes one atmospheric pressure, $L_0$ is the Loschmidt constant, $\bar{\nu}_{rbg}$ the average relative velocity of the Cs and buffer gas atoms, $\sigma_{2bg}$ the Cs–buffer gas collision cross section, and $\gamma_{se}$ the coherence spin exchange relaxation rate. The first term on the right-hand side in expression (3) represents the collision relaxation of Cs–Cs atoms and the Cs-cell inner wall, and it decreases with the increase in buffer gas partial pressure $P$ (the first term on the right-side, $P_0/P$). The second term represents the relaxation of Cs atoms with the collision of buffer gas atoms, and it increases with the increase in buffer gas partial pressure $P$ (the second term on the right-side, $P/P_0$). The third term refers to the spin exchange relaxation, which can be ignored at room temperature. Therefore, at moderate pressures, the first term plays a major role. The buffer gas will reduce Cs atoms diffusing to the cell wall, and at high pressures, the Cs–buffer gas (the second term) collision dominates the coherence relaxation rate.

For our Cs–Ne vapor cells at the moderate pressure, $\gamma$ is determined mainly by the first term, whereas the buffer gas reduces transit time broadening. In other words, the Cs–buffer gas collision reduces the rate of Cs atom diffusion and Cs-cell wall collision, so the relaxation rate $\gamma$ of the two hyperfine levels in the Cs ground state decreases. Therefore, the population time of the atoms in the coherent dark state grows, and the linewidth of the CPT spectrum decreases (Fig. 3). The results are in qualitative agreement with those obtained from Eq. (1).

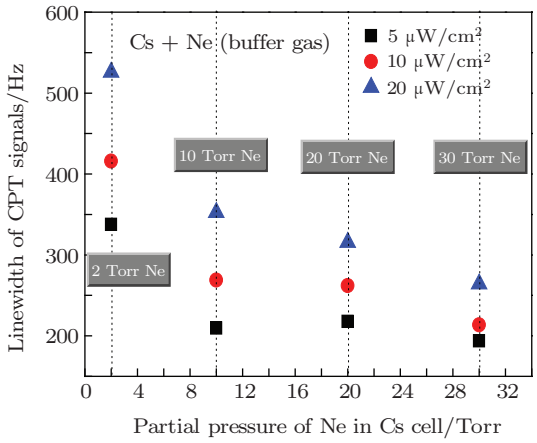



**Fig. 3.** (color online) The linewidth values of the CPT resonance peak versus Ne partial pressure at room temperature.

The CPT resonance shape and linewidth versus the total light intensity were investigated in Refs. [19] and [21]. We also measure the linewidth and amplitude of the CPT signal versus the light intensity for four different Cs–Ne cells in order to extract new points (Figs. 4(a) and 4(b)).

According to the (1) and (2) formulas, substituting the Rabi angular frequency with $\omega_R = 2\pi \cdot \Gamma^* \sqrt{I/2I_s}$, and $I_{ML} = I_{SL} = I$, we have

$$\Delta\upsilon = \frac{1}{\pi}\left(\gamma + \frac{2\pi^2 \cdot \Gamma^* \cdot I}{I_s}\right), \tag{4}$$

$$S \propto \frac{4\pi^4 \cdot \Gamma^{*3} \cdot I^2}{I_s^2} \cdot \frac{1}{\gamma + \dfrac{2\pi^2 \cdot \Gamma^* \cdot I}{I_s}}. \tag{5}$$

For any one of the selected Cs vapor cells, it can be seen that the decay rate $\Gamma^*$ and the saturation intensity $I_s$ are constants, and only the laser intensity is variable. It is obvious that the linewidth of the CPT resonance transmission peak is linearly dependent on the light intensity (Fig. 4(a) is consistent with Eq. (4)). The increasing rate is reflected by the slope, which is affected by the partial pressure of the buffer gas. When the buffer gas partial pressure increases, the slope decreases, which means that the buffer gas reduces the sensitivity of the CPT linewidth for the light intensity, and effectively restricts power broadening. In Fig. 4(a), if the CPT linewidth is extrapolated to zero light intensity, according to Eq. (4), we have $\Delta\upsilon = \gamma/\pi$. It is also possible to estimate the ground state relaxation rate $\gamma$ and the decoherence time $\tau$ ($\tau = 1/\gamma$) of any Cs vapor cell (Table 1). Therefore, buffer gas can significantly prolong decoherence time between the ground states, suppress power broadening, narrow the linewidth, and improve the signal-to-noise ratio.

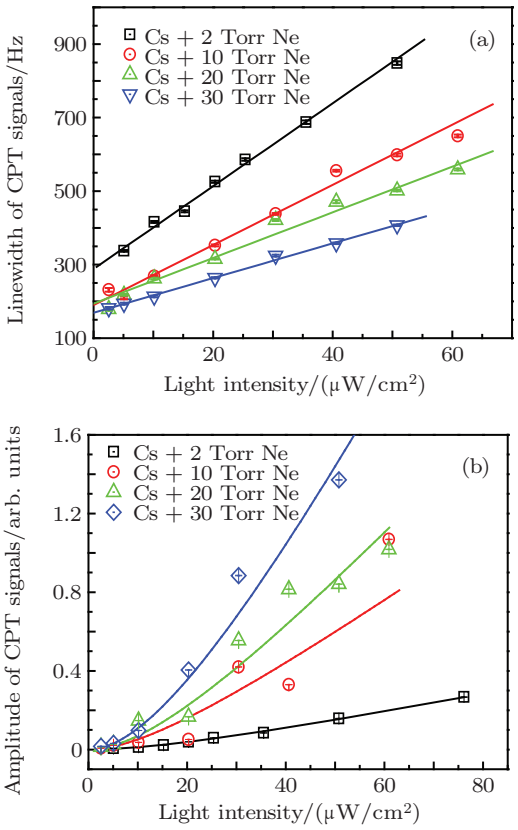



**Fig. 4.** (color online) Plots of the linewidth and amplitude of the CPT signal versus laser intensity for four Cs–Ne cells with different partial pressure Ne at room temperature. The points are measured data, while the solid lines are theoretical fitting according to Eqs. (1) and (2). The laser intensities of the two coherent laser beams are equal, and the Cs–Ne vapor cell is placed in the magnetic shielding tank with a residual magnetic field of $\sim 1$ nT.

**Table 1.** Estimated characteristics of Cs–Ne cells at room temperature according to Fig. 3(a) and our previous work.[6] The size of the Cs cell is $\phi$25 mm×75 mm.

| Partial pressure of Ne gas/Torr | CPT linewidth ($\gamma/\pi$) at zero intensity/Hz | Decoherence time $\tau$/ms |
|---|---|---|
| 0 | 17000 | 0.02 |
| 2 | 290.3 | 1.10 |
| 10 | 186.4 | 1.71 |
| 20 | 194.9 | 1.63 |
| 30 | 169.5 | 1.88 |

### 3.2. The frequency shift versus the partial pressure of Ne buffer gas

Although the buffer gas has many good aspects for the CPT spectrum, at the same time it brings a frequency shift of CPT resonance.[17] The shift in the central frequency of the CPT resonance transmission peak is plotted as a function of the partial pressure of Ne buffer gas at room temperature in Fig. 5. The resonance shift increases linearly with rising Ne partial pressure. A linear fitting gives a frequency shift rate of $\sim$ 570 Hz/Torr (4.3 Hz/Pa) (theoretically, the actual buffer gas pressure in the sealed cell can be roughly estimated through the CPT frequency shift). There are two possible reasons for this: one is the collision between the buffer gas and the Cs atoms, which leads to an atomic hyperfine frequency shift, so that the frequency of the coherent states shift, and the other is the collision that only makes the coherent state frequency shift, but does not affect the Cs atomic level. Therefore, we conduct the following testing experiment.

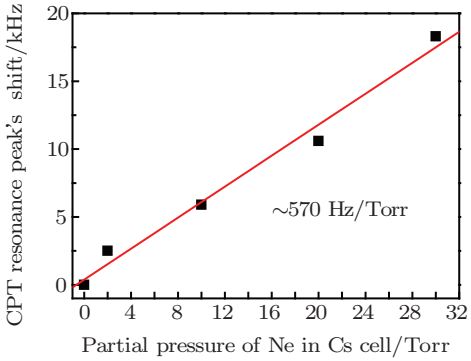



**Fig. 5.** (color online) The frequency shift of the CPT resonance peak as a function of Ne partial pressure at room temperature.

A laser with a wavelength of 852 nm passes through the Cs atomic vapor cell singly. Scanning laser current and Cs atomic absorption spectroscopy are observed (Fig. 6). We note that on the $x$ axis, the frequency (the diode current) increases (decreases) rightwards. The frequency difference between the peaks of pure Cs is given by the well-known hyperfine structure of the two ground states of Cs (9.19263177 GHz), which serves as a ruler to calibrate the $x$ axis. Because the energy intervals of the excited states are less than the Doppler broadening, we cannot see the absorption peak of the hyperfine transition. The laser beam diameter is about 2 mm and the power

is about 90 μW. We use four different atomic cells with the same dimensions ($\phi$25 mm×75 mm). Of them, one is a pure Cs vapor cell, and three cells are additionally filled with 10, 20, and 30 Torr (1.3 kPa, 2.7 kPa, 4 kPa) Ne as the buffer gas, respectively.

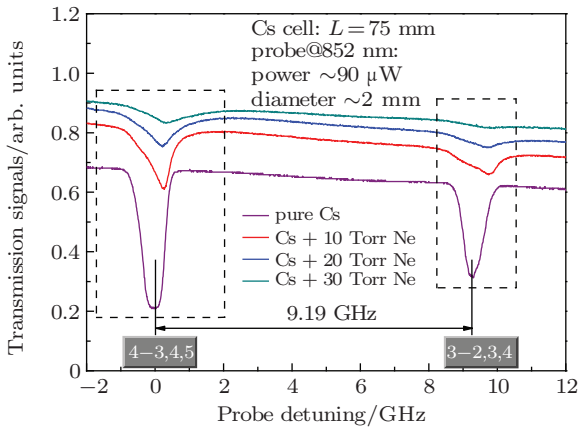



**Fig. 6.** (color online) The absorption spectra for a pure Cs vapor cell and three Cs vapor cells filled additionally with different partial pressures of Ne. The absorption peaks are shifted by the buffer gas (Ne). The longitudinal coordinates of the curves for different atomic cells are shifted in order to distinguish them. The inclined backgrounds are due to the residual variation in laser output power when scanning the probe laser frequency by scanning the laser diode injection current. The dashed boxes represent the same transitions (Cs $6S_{1/2}$ $F_g = 4$–$6P_{3/2}$ $F_e = 3$, 4, 5 transitions for the left and Cs $6S_{1/2}$ $F_g = 3$–$6P_{3/2}$ $F_e = 2$, 3, 4 transitions for the right).

From Fig. 6 we can see that the absorption peaks in the Cs–Ne vapor cells are significantly reduced as the neon partial pressure ratio increases. It seems that the single-photon absorption is weakened, thereby improving the signal-to-noise ratio of the CPT resonance peak (Fig. 4(b)). In addition, we can also see the central frequency of the Doppler absorption peak and CPT resonance transmission peak shift toward the same direction (the high frequency), which is more and more obvious as the neon partial pressure ratio increases. Therefore, we can conclude that the collision between the Cs and Ne induces the Cs atomic energy levels to shift, and not only the ground states but also the coherent superposition dark state of the ground state is shifted.

However, optimizing the partial pressure ratio of two kinds of buffer gases that have opposite frequency-shift coefficients (Ar–Ne or $CH_4$–$N_2$) can minimize or eliminate the frequency shift.[22] This will then reduce the temperature sensitivity of the CPT resonance frequency.[23] The above-mentioned experimental results and discussion will be helpful for improving the frequency stability of CPT atomic clocks.

## 4. Conclusions

We measured and discussed the good and bad influences of buffer gas (here, Ne) partial pressure on the coherent population trapping resonance in Cs vapor cells around room temperature. We found that a suitable partial pressure buffer gas can effectively narrow the CPT linewidth and improve the signal amplitude, and that introducing the buffer gas with opposite frequency-shift coefficients can eliminate central frequency shift. This will be helpful in improving the frequency stability of CPT atomic clocks and the sensitivity of CPT atomic magnetometers.

## References

[1] Alzetta G, Gozzini A, Moi L and Orriols G 1976 *Nuovo Cimento B* **36** 5
[2] Aspect A, Arimondo E, Kaiser R, Vansteenkiste N and Cohen-Tannoudji C 1988 *Phys. Rev. Lett.* **61** 826
[3] Scully M O and Fleischauer M 1992 *Phys. Rev. Lett.* **69** 1360
[4] Liu G B, Du R C, Liu C Y and Gu S H 2008 *Chin. Phys. Lett.* **25** 472
[5] Pradhan S, Behera R and Das A K 2012 *Appl. Phys. Lett.* **100** 173502
[6] Vanier J, Godone A and Levi F 1998 *Phys. Rev. A* **58** 2345
[7] Knappe S, Shah V, Schwindt P D D, Hollberg L, Kitching J, Liew Li-Anne and Moreland J 2004 *Appl. Phys. Lett.* **85** 1460
[8] Su J, Deng K, Guo D Z, Wang Z, Chen J, Zhang G M and Chen X Z 2010 *Chin. Phys. B* **19** 110701
[9] Du R C, Chen J W, Liu C Y and Gu S H 2009 *Acta Phys. Sin.* **58** 6117 (in Chinese)
[10] Liu L, Guo T, Deng K, Liu X Y, Chen X Z and Wang Z 2007 *Chin. Phys. Lett.* **24** 1883
[11] Yang J, Liu G B and Gu S H 2012 *Acta Phys. Sin.* **61** 043202 (in Chinese)
[12] Deng J L, Hu Z F, He H J and Wang Y Z 2006 *Chin. Phys. Lett.* **23** 1745
[13] Liu Z, Diao W T, Wang J Y, Liang Q B, Yang B D, He J, Zhang T C and Wang J M 2012 *Acta Phys. Sin.* **61** 233201 (in Chinese)
[14] Liu G B, Zhao F and Gu S H 2009 *Chin. Phys. B* **18** 3839
[15] Unks B E, Proite N A and Yavuz D D 2007 *Rev. Sci. Instrum.* **78** 083108
[16] Yun P, Tan B Z, Deng W and Gu S H 2011 *Rev. Sci. Instrum.* **82** 123104
[17] Brandt S, Nagel A, Wynands R and Meschede D 1997 *Phys. Rev. A* **56** 1063
[18] Chen W L, Qi X H, Yi L, Deng K, Wang Z, Chen J B and Chen X Z 2008 *Opt. Lett.* **33** 357
[19] Moon H S, Park S E, Park Y H, Lee L and Kim J B 2006 *J. Opt. Soc. Am. B* **23** 2393
[20] Diao W T, He J, Liu Z, Yang B D and Wang J M 2012 *Opt. Express* **20** 7480
[21] Boudot R, Dziuban P, Hasegawa M, Chutani R K, Galliou S, Giordano V and Gorecki C 2011 *J. Appl. Phys.* **109** 014912
[22] Pitz G A, Wertepny D E and Perram G P 2009 *Phys. Rev. A* **80** 062718
[23] Deng K, Guo T, He D W, Liu X Y, Liu L, Guo D Z, Chen X Z and Wang Z 2008 *Appl. Phys. Lett.* **92** 211104